MULTIPLE IMAGE MATCHING

Peggy Agouris
Toni Schenk

Department of Geodetic Science and Surveying
The Ohio State University, Columbus, Ohio 43210-1247
USA

Commission III

ABSTRACT

Digital photogrammetry is concerned with the development of algorithms to automate photogrammetric tasks. The majority of efforts though are focused on single stereopairs. This paper addresses the task of simultaneously matching conjugate windows from multiple overlapping images. After establishing a theoretical understanding of the problem, we introduce several approaches and present the associated mathematical principles. We report on the advantages and disadvantages of each one, discuss various implementation issues and in conclusion, we examine potential applications in photogrammetric procedure.

1. INTRODUCTION

Digital photogrammetry has recently emerged as one of the most promising and multi-faceted photogrammetric subfields. A solid body of research work and a wide array of topics have laid the foundation for the evolution of the photogrammetric procedure. Among the research topics, automatic matching is one of the most challenging.

Digital image matching attempts to identify sets of conjugate entities from two or more overlapping images. From the diverse set of matching techniques [Lemmens, 1988], least squares matching is a popular choice [Ackerman, 1984]. Even though there already exists substantial work on this subject, most efforts have been focused on the stereomatching case, which involves a single pair of images. This paper deals with simultaneously matching windows from multiple overlapping images using least squares techniques. The significance of this issue lies in the impracticality of handling single models at the time when processing large blocks is common practice in the photogrammetric industry. Successful and efficient completion of multiple image matching is expected to contribute significantly in the transition of digital photogrammetry from an experimental to a production-oriented status.

Significant research in the area of multiple image matching can be found in [Grün & Baltsavias, 1988],[Heipke, 1992] and [Helava, 1988]. In this paper, we present alternative approaches to the subject by introducing geometric constraints and performing matching in the object space. The general least squares matching procedure is discussed in detail and is subsequently expanded to accommodate multiple image windows. We explore the theoretical issues of the proposed approaches and establish the corresponding mathematical principles. Then, we report on their advantages and disadvantages from a photogrammetric point of view and address several implementation issues.

2. LEAST SQUARES MATCHING

Least squares matching techniques attempt to match windows of pixels by establishing a correspondence between them which minimizes the differences of their gray values. Assuming $g_L(x_L, y_L)$ to be a window of $n_1 \times n_2$ pixels in the left image, and $g_R^\circ(x_R^\circ, y_R^\circ)$ an equal size approximation to its conjugate position in the right image, the objective is to estimate a new location of the right image window $g_R(x_R, y_R)$ such that the gray value differences

$$g_L(x_L, y_L) - g_R(x_R, y_R) = e(x, y) \tag{1}$$

are minimized. The estimation is performed by the transformation of the coordinates (x_R°, y_R°) and resampling of the corresponding gray values. The coordinates of the two windows are related through a perspective transformation to a common surface patch in the object space. Taking into account the very small size of the windows to be matched, their coordinates are assumed to be related to each other by a 6-parameter affine transformation

$$x_R = a_1 + a_2 x_L + a_3 y_L \tag{2}$$

and

$$y_R = b_1 + b_2 x_L + b_3 y_L \tag{3}$$

With linearization, the equations

$$g_L(x_L, y_L) - e(x, y) = g_R^\circ(x_R^\circ, y_R^\circ) \tag{4}$$

become

$$g_L(x_L, y_L) - e(x, y) = g_R^\circ(x_R^\circ, y_R^\circ) + g_{R_x} dx_R + g_{R_y} dy_R \tag{5}$$

with the terms g_{R_x} and g_{R_y} expressing the local gradient of the right image function in the x and y direction respectively as

$$g_{R_x} = \frac{\partial g_R^o(x_R^o, y_R^o)}{\partial x_R} \quad \text{and} \quad g_{R_y} = \frac{\partial g_R^o(x_R^o, y_R^o)}{\partial y_R} \tag{6}$$

By differentiating and substituting the affine transformation parameters, the observation equations become

$$\begin{aligned} g_L(x_L, y_L) - e(x,y) &= g_R^o(x_R^o, y_R^o) + g_{R_x} da_1 + g_{R_x} x_L da_2 \\ &+ g_{R_x} y_L da_3 + g_{R_y} db_1 + g_{R_y} x_L db_2 \\ &+ g_{R_y} y_L db_3 \end{aligned} \tag{7}$$

One observation equation is formed for every pair of pixels from the left and right image templates, resulting in a total of $n_1 \cdot n_2$ equations for templates of size $n_1 \times n_2$. Using matrix notation we have

$$-e = Ax - l \tag{8}$$

where the vector of unknowns x is

$$x^T = [da_1, da_2, da_3, db_1, db_2, db_3] \tag{9}$$

and each element of the vector of observations l is of the form

$$l = g_L(x_L, y_L) - g_R^o(x_R^o, y_R^o) \tag{10}$$

while each line of the design matrix A is

$$A = [g_{R_x}, g_{R_x} x_L, g_{R_x} y_L, g_{R_y}, g_{R_y} x_L, g_{R_y} y_L] \tag{11}$$

The least squares solution is

$$x = (A^T P A)^{-1} A^T P l \tag{12}$$

with P the associated, typically diagonal, weight matrix. By using the transformation parameters obtained through the least squares solution to update the coordinates and resample gray values at integer grid coordinates, a new right image window $g_R^1(x_R^1, y_R^1)$ centered at

$$x_R^1 = (a_1^o + da_1) + (a_2^o + da_2) x_L + (a_3^o + da_3) y_L \tag{13}$$

and

$$y_R^1 = (b_1^o + db_1) + (b_2^o + db_2) x_L + (b_3^o + db_3) y_L \tag{14}$$

is selected as conjugate of the stationary left image template $g_L(x_L, y_L)$. A new set of observation equations is formed and solved. In this manner, the true conjugate window $g_R(x_R, y_R)$ is identified as the window $g_R^n(x_R^n, y_R^n)$ at which the least squares iterated solution is converging. It is common practice to use least squares matching as a means for identifying conjugate points rather than windows. Thus, we correspond the point (x_R^n, y_R^n), center of the right image window, to the point (x_L, y_L) of the left image. The maximum allowable pixel coordinate difference between the initial approximation and the final solution for which the technique can still converge is termed pull-in range.

The great advantage of least squares matching is its flexibility and the fact that it is a well-known and documented technique. The basic model which has been described here can easily be expanded to accommodate more than two images or to include various additional constraints. Radiometric parameters can also be included in an effort to compensate for differences in brightness and contrast between the two images, and are particularly helpful when using digitized images of analog diapositives [Pertl, 1985]. However, a radiometric adjustment is typically performed prior to the least squares solution, equalizing the average and the standard deviation of gray values of the two conjugate windows, thus accommodating for uneven radiometric properties of the two images.

3. MULTIPLE IMAGE LEAST SQUARES MATCHING

3.1 Mathematical Formulation for Multiple Images

Multiple image matching can be performed by simultaneously minimizing the gray value differences between all the possible pairs of conjugate image windows. One image window has to be kept constant and serves as the matching template. For every pair of conjugate image windows (w_i, w_j), depicting the same object-space area in the overlapping photos i and j, we form the observation equations

$$g_i(x_i, y_i) - g_j(x_j, y_j) = e_{ij}(x, y) \tag{15}$$

For windows of $n_1 \times n_2$ pixels appearing in n overlapping photographs we have a total of $(n-1) + (n-2) + \ldots + 2 + 1 = \frac{n(n-1)}{2}$ pairs of conjugate image windows and therefore $\frac{n(n-1)}{2} n_1 n_2$ observation equations. According to the general least squares matching approach, each pair of conjugate windows is geometrically related through a six-parameter affine transformation

$$x_j = a_1^{ij} + a_2^{ij} x_i + a_3^{ij} y_i \tag{16}$$

$$y_j = b_1^{ij} + b_2^{ij} x_i + b_3^{ij} y_i \tag{17}$$

or, conceptually

$$(x_j, y_j) = f^{ij}(x_i, y_i) \tag{18}$$

However, we cannot introduce a set of affine transformation parameters for every pair of image windows since that leads to dependency between transformation parameters. Instead, we can use the set of transformation parameters relating each window w_i to the template window w_1

$$(x_i, y_i) = f^{1i}(x_1, y_1) \qquad \text{for} \quad i = 2, 3 \ldots n \tag{19}$$

which uniquely and sufficiently describes the geometric relationships between all possible conjugate window pairs [Tsingas, 1991]. Indeed, the transformation between a window w_j in photo j and its conjugate window w_i in photo i is uniquely described through the parameters relating each window to the template window w_1 as

$$(x_j, y_j) = f^{1j}(f^{1i})^{-1}(x_i, y_i) \tag{20}$$

with the inverse affine transformation $f^{i1} = (f^{1i})^{-1}$ defined as

$$x_1 = \frac{b_3^{1i} a_1^{1i} - b_1^{1i} a_3^{1i}}{a_3^{1i} b_2^{1i} - a_2^{1i} b_3^{1i}} + \frac{-b_3^{1i}}{a_3^{1i} b_2^{1i} - a_2^{1i} b_3^{1i}} x_i + \frac{a_3^{1i}}{a_3^{1i} b_2^{1i} - a_2^{1i} b_3^{1i}} y_i \tag{21}$$

$$y_1 = \frac{a_2^{1i} b_1^{1i} - b_2^{1i} a_1^{1i}}{a_3^{1i} b_2^{1i} - 1_2^{1i} b_3^{1i}} + \frac{b_2^{1i}}{a_3^{1i} b_2^{1i} - a_2^{1i} b_3^{1i}} x_i + \frac{-a_2^{1i}}{a_3^{1i} b_2^{1i} - a_2^{1i} b_3^{1i}} y_i \tag{22}$$

Substituting in equations

$$x_j = a_1^{1j} + a_2^{1j} x_1 + a_3^{1j} y_1 \tag{23}$$

$$y_j = b_1^{1j} + b_2^{1j} x_1 + b_3^{1j} y_1 \tag{24}$$

x_1 and y_1 from equations 21 and 22 we can rewrite the affine transformation relating windows w_i and w_j (equations 16 and 17) as a function of the two sets of parameters which relate each window to the template.

Proceeding further according to conventional least squares approach, we have a total of $6(n-1)$ statistically independent transformation parameters, relating each image window w_i $(i = 2, 3, \ldots n)$ to the reference template. Therefore the dimensions of the associated vector of unknowns

$$x^T = [da_1^{12}, da_2^{12}, \ldots db_2^{1n}, db_3^{1n}] \tag{25}$$

will be $6(n-1) \times 1$. Each set of observation equations (equation 15) must be linearized as following

$$\begin{aligned} g_i(x_i, y_i) - e(x, y) &= g_j^o(x_j^o, y_j^o) + g_{j_x} \frac{\partial x_j}{\partial a_1^{1j}} da_1^{1j} + \ldots \\ &+ \ldots + g_{j_y} \frac{\partial y_j}{\partial b_3^{1j}} db_3^{1j} + g_{j_x} \frac{\partial x_j}{\partial a_1^{1i}} da_1^{1i} + \ldots \\ &+ \ldots + g_{j_y} \frac{\partial y_j}{\partial b_3^{1i}} db_3^{1i} \end{aligned} \tag{26}$$

Each pair of pixels from every pair of windows produces one observation equation. Among the $\frac{n(n-1)}{2}$ distinct pairs of conjugate windows, there exist $(n-1)$ pairs relating each window w_i $(i = 2, 3, \ldots n)$ to the reference template w_1. Observation equations formed by these pairs will only produce six nonzero elements for each line of the coefficient matrix A, at the columns which correspond to the parameters of the f^{1i} affine transformation. Observation equations relating two windows w_i and w_j $(i \neq j \neq 1)$ will produce twelve nonzero elements per line, at the columns corresponding to the parameters of both the f^{1i} and f^{1j} affine transformations. The sparsity pattern of the design matrix A for the case of five conjugate windows is shown in Fig. 1. The dimensions of each block of nonzero elements (gray square) are $(n_1 \cdot n_2) \times 6$, while the parameters are ordered as $f^{12}, \ldots f^{15}$ and the observations as $1-2, 1-3, \ldots, 1-5, 2-3, \ldots, 4-5$. The least squares solution is again

$$x = (A^T P A)^{-1} A^T P l \tag{27}$$

and the final solution is obtained after iterations. The normal matrix $(A^T P A)$ is full but the exploitation of the sparsity patterns of matrix A can facilitate computations and storage requirements.

3.2 Introduction of Geometric Constraints

The previously described technique attempts to match multiple images using solely the recorded gray values, without imposing any geometric constraints on the relative position of overlapping images in the object space. By simply using the affine transformation as the geometric relationship between two or more conjugate windows, their geometric interdependence, as expressed by the satisfaction of the collinearity condition equations, is not taken into consideration. Therefore, this approach just minimizes gray value differences without enforcing a geometrically coherent solution. Windows displaying sufficient radiometric similarity can be matched even though their parallax values may be unacceptable. This problem can be overcome either by checking the resulting parallax values or, in a more robust fashion, by introducing geometric constraints within the solution process itself.

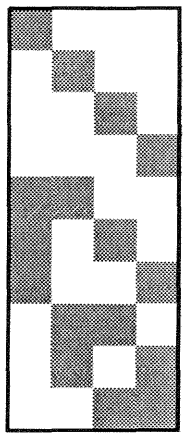

Figure 1: Sparsity pattern of the design matrix for multiple image least squares matching without additional constraints

Geometric constraints can be introduced either as additional equations [Grün & Baltsavias, 1988], or by properly modifying the expression which relates the coordinate systems of conjugate windows. The image coordinates (x_P^j, y_P^j) (reduced to principal point) of a point $P(X_P, Y_P, Z_P)$ of the object space in photo j satisfy the collinearity condition

$$\begin{bmatrix} x_P^j \\ y_P^j \\ -c \end{bmatrix} = \frac{1}{\lambda_P^j} R^j \begin{bmatrix} X_P - X_o^j \\ Y_P - Y_o^j \\ Z_P - Z_o^j \end{bmatrix} \tag{28}$$

or, in matrix notation

$$\vec{x_P^j} = \frac{1}{\lambda_P^j} R^j (\vec{X_P} - \vec{X_o^j}) \tag{29}$$

where R_j the rotation matrix of image j, $\vec{X_o^j}$ the ground coordinates of the exposure center of photo j and λ_P^j the associated scale factor.

Backsolving the collinearity condition for the image of the same point P in photo i we obtain

$$\vec{X_P} = \lambda_P^i R_i^T \vec{x_P^i} + \vec{X_o^i} \tag{30}$$

and substituting this expression of $\vec{X_P}$ into equation (29) gives

$$\vec{x_P^j} = \frac{\lambda_P^i}{\lambda_P^j} R_j R_i^T \vec{x_P^i} + \frac{1}{\lambda_P^j} R_j (\vec{X_o^i} - \vec{X_o^j}) \tag{31}$$

in which we have two expressions (one for x and and one for y) relating the (x_P^j, y_P^j) image coordinates of point P in photo j to the (x_P^i, y_P^i) image coordinates of the same point in photo i, as a function of the exterior orientation parameters of both photos. Conceptually, in accordance to equation 18, by expanding the equation over pairs of window coordinates (w_i, w_j) and dropping the index P we have

$$(x_j, y_j) = \phi^{ij}(x_i, y_i) \tag{32}$$

with ϕ being the above described function. This function should be considered the object space equivalent of equation 20 rather than equation 18 since the relationship between a pair of windows is described through their relationship to a reference window, which in this case is the object space patch.

By using all potential unique permutations of photo pairs as observation equations, and using one window as the radiometric reference template, as previously described in section 3.1, we can form up to $\frac{n(n-1)}{2}$ distinct pairs of conjugate windows, or $\frac{n(n-1)}{2}n_1n_2$ corresponding observation equations. Each observation equation (equation 15) can be linearized with respect to any preselected set of m orientation parameters per photo $(o_1^i, \ldots, o_m^i, o_1^j, \ldots, o_m^j)$ as

$$\begin{aligned} g_i(x_i, y_i) - e(x, y) &= g_j^o(x_j^o, y_j^o) + g_{j_x}\frac{\partial x_j}{\partial o_1^i}do_1^i + \ldots \\ &+ \ldots + g_{j_y}\frac{\partial y_j}{\partial o_m^i}do_m^i + g_{j_x}\frac{\partial x_j}{\partial o_1^j}do_1^j + \ldots \\ &+ \ldots + g_{j_y}\frac{\partial y_j}{\partial o_m^j}do_m^j \end{aligned} \quad (33)$$

The reference template (in photo 1) has to be kept stable, therefore the exterior orientation parameters of photo 1 will be kept constant during the matching process. Thus, the solution can be considered the digital equivalent of dependent analog orientation. Since the original model is non-linear, the final solution is obtained through iterations. The design matrix for this case will have similar sparsity pattern to the one shown in Fig. 1, but the dimensions of each block of nonzero elements will be $(n_1 \cdot n_2) \times m$. After each iteration, the image coordinates of point P in photo j are updated due to changes in orientation parameters

$$x_j = x_j^o + \frac{\partial x_j}{\partial o_1^j}do_1^j + \ldots + \frac{\partial x_j}{\partial o_m^j}do_m^j \quad (34)$$

and

$$y_j = y_j^o + \frac{\partial y_j}{\partial o_1^j}do_1^j + \ldots + \frac{\partial y_j}{\partial o_m^j}do_m^j \quad (35)$$

By solving the above system we inherently ensure that conjugate image rays intersect at a point in the object space. While plain least squares matching is solely a radiometric adjustment, the use of object space constraints to express the relationship of two or more conjugate windows allows the combination of the radiometric and geometric solutions in a single adjustment procedure. The model can be expanded to include the object space coordinates of point P which can be introduced into the adjustment by properly expressing the scale factors as functions of them. In addition, the technique can be expanded to simultaneously adjust observations of more than one point in the object space. The images of all points in each photo will be related through a common set of exterior orientation parameters and the adjustment can thus proceed in a global manner.

3.3 Matching in the Object Space

By examining the image formation process we can extract some rules which can later be used in the matching process not only as constraints but also to expand the problem into the radiometric and/or geometric reconstruction of the object space itself.

Fig. 2 shows four image windows $w_1, \ldots w_4$ displaying approximately the same surface patch S in four overlapping images. The surface is described by two continuous functions, one geometric $Z(X,Y)$ (elevations) and another radiometric $G(X,Y)$ (gray values). Assuming a local tesselation, whereby the surface patch S is represented as a Digital Elevation and Radiometry Model ($DERM$, a term analogous to DEM) with a resolution of $n_1 \times n_2$ grid points, the patch is defined by $n_1 \cdot n_2$ elevations and by an equal number of gray values. The reconstruction of the patch would therefore involve the determination of these $2 \cdot n_1 \cdot n_2$ parameters. These parameters can be determined by defining the geometric and radiometric transformations which relate S to its images $w_1, \ldots w_4$. Each image window w_i corresponds to a gray value function $g_i(x_i, y_i)$, related to S through a geometric transformation

$$(x_i, y_i) = T_g^i(X, Y, Z) \quad (36)$$

and a radiometric one

$$g_i(x_i, y_i) = T_r^i[G(X, Y)] \quad (37)$$

Assuming the object space patch S to be a Lambertian surface, the recorded image irradiance $g(x,y)$ (image gray values) is directly related to the surface radiance $G(X,Y)$ (surface patch gray levels). Furthermore, taking into account the relatively small size of the surface patch, the rather complex radiometric relationship between image and object space can be effectively approximated by a linear transformation

$$g_i(x, y) = r_0^i + r_1^i G(X, Y) \quad (38)$$

Assuming a Lambertian light source, the values of the radiometric shift (r_0^i) and scale (r_1^i) parameters are unique for each image and they are functions of the surface albedo as well as of the angles formed between the image window w_i and the normal to the surface [Horn, 1986].

The radiometric adjustment is typically performed prior to the matching process, by forcing each window w_i to have the same average and standard deviation of gray values as the reference template w_1. Thus, we actually force

$$r_0^i = r_0^1 = r_0 \quad \text{and} \quad r_1^i = r_1^1 = r_1 \quad (39)$$

Subsequently, the gray values $g_1(x_1, y_1)$ of w_1 are assigned to the surface patch S. The assignment can be performed either directly:

$$G(X, Y) = g_1(x_1, y_1) \quad (40)$$

or through an inverse linear transformation

$$G(X, Y) = \frac{g(x, y) - r_0}{r_1} \quad (41)$$

In order for an inverse linear transformation to be used, the parameters r_0 and r_1 have to be determined using a priori

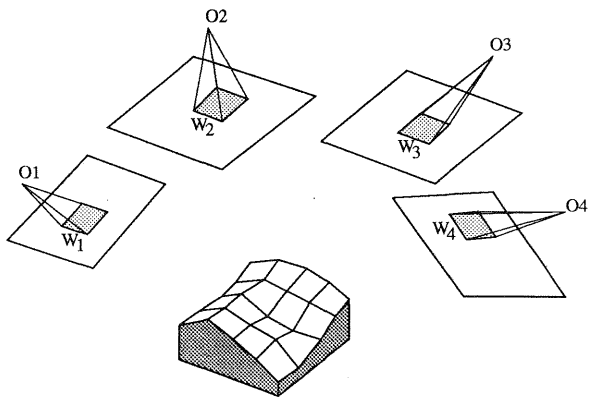

Figure 2: Overlapping image windows in the object space

knowledge on the surface radiance, while for the correct assignment of gray values we must have some approximations of image orientation.

Assuming a smooth surface and no extreme variations in exposure geometry, we can accept an one-to-one correspondence between the object space tesselation and the image windows. Therefore, the observation equations which were developed in the previous sections can now be formed using the object space as the reference template

$$G(X,Y) - g_i(x_i, y_i) = e(x,y) \tag{42}$$

thus transferring the matching procedure to the object space. The geometric relationship between the image coordinates (x_i, y_i) of a point in photo i and its object space coordinates (X, Y, Z) will be in general a seven-parameter transformation

$$(x_i, y_i) = \xi^i(X, Y, Z) \tag{43}$$

This transformation need not be the collinearity condition, as long as the seven parameters which describe the three translations, three rotations and one scale factor are linearly independent. Some of the transformation parameters may also be kept constant during the adjustment, if a priori information allows us to consider them known.

In order for the elevation values to be computed through the adjustment, they have to be introduced as adjustable quantities. This can be performed by proper selection of the other six transformation parameters $(p_1^i, \ldots p_6^i)$ to avoid dependencies which would lead to ill-conditioned systems. The linearized observation equations for this case are

$$\begin{aligned} G(X,Y) - e(x,y) &= g_i^o(x_i^o, y_i^o) + (g_{i_x}\frac{\partial x_i}{\partial p_1^i} + \\ &+ g_{i_y}\frac{\partial y_i}{\partial p_1^i})dp_1^i + \ldots + (g_{i_x}\frac{\partial x_i}{\partial p_6^i} + \\ &+ g_{i_y}\frac{\partial y_i}{\partial p_6^i})dp_6^i + (g_{i_x}\frac{\partial x_i}{\partial Z} + \\ &+ g_{i_y}\frac{\partial y_i}{\partial Z})dZ \end{aligned} \tag{44}$$

Taking into account that different pixels in the image window w_i correspond to different elements of the ground tesselation (groundels, [Helava, 1988]), we see that the dZ element of the above equation is actually a vector of $n_1 \cdot n_2$ elements. Thus, the design matrix A of the adjustment solution will have the sparsity pattern shown in Fig. 3. In this figure, the large gray blocks have dimensions $(n_1 \cdot n_2) \times 6$, while the small black blocks indicate single entries. This pattern corresponds to the four overlapping images of Fig. 2, without using observations in between windows. Window w_1 has been projected to the object space during the radiometric adjustment and the observations relate the surface patch S to the windows w_2, w_3 and w_4. A more detailed description and in-depth analysis of this technique can be found in [Schenk & Toth, 1992].

Conceptually, object space matching resembles matching with geometric constraints. Taking into account the fact that all images are created from the same object space patch, least squares matching is enforced to produce a geometrically acceptable solution. Simultaneously, we are able to reconstruct the object space $DERM$. Considering that one photo is used to create the object space patch, it is clear that this technique is equivalent to dependent orientation.

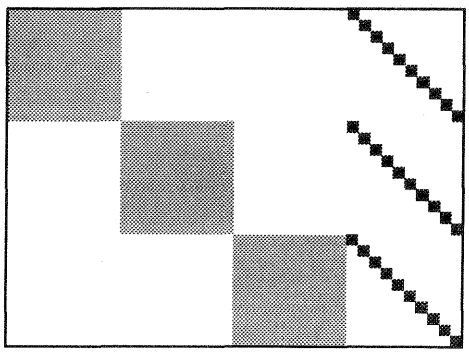

Figure 3: Sparsity pattern of the design matrix for object space matching

4. IMPLEMENTATION ISSUES

In the previous sections we presented and analyzed the formulation of least squares matching using multiple images. By introducing geometric constraints and performing matching in the object space, consistent matching results can be ensured and surface patches can be reconstructed geometrically as well as radiometrically.

Approximations are obviously necessary and they can be in the form of conjugate point image coordinates, orientation parameters and/or the object space surface, as expressed by, e.g., an initial DEM approximation. These approximations can be easily obtained through an automatic stereopair orientation module [Schenk et al., 1991]. Experiments have shown that accuracies of the order of $\frac{1}{10}$ to $\frac{1}{15}$ of a pixel (or $4 - 6\mu m$ in photo coordinates) are to be expected when the technique is applied as a combination of feature-based hierarchical matching and correlation methods with continuous updating of the results through scale space [Stefanidis et al., 1991].

Automatic stereopair orientation and least squares multiphoto matching can be ideally combined in automatic aerotriangulation of large blocks of images, the former providing valid initial approximations and the latter, being the core module of the procedure, performing precise point determination. This fusion of more than one module should be expected, since initial approximations are required in aerotriangulation. Stereopair orientation essentially performs automatically the task of selecting conjugate image windows located in the areas where conjugate points are desired, the equivalent of the preparation phase in the conventional aerotriangulation procedure. Using these initial matching approximations, the images are approximately brought in their correct relative positions in space. This can be visually materialized for operator inspection, if desired, through the generation and continuous updating of a photomosaic. Fig. 3 depicts a photomosaic of three images, an early product of the automatic aerotriangulation procedure. The simultaneous multiphoto matching technique can also be conceptually viewed as the digital equivalent of an n-stage comparator, allowing for the measurement of conjugate points in more than two images at a time. Several gross errors, associated with erroneous conjugate point identification, which limit the accuracy of conventional analytical aerotriangulation can thus be avoided, optimizing the potential accuracies of the technique.

By using a feature-driven stereomatching method to obtain

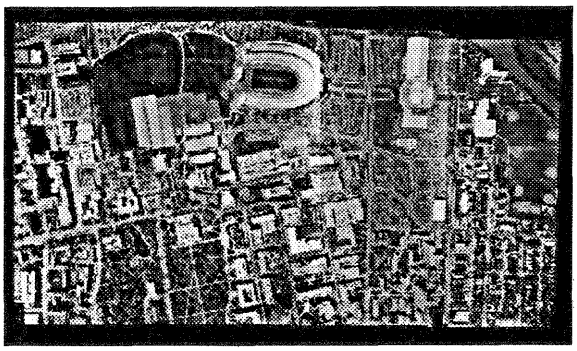

Figure 4: A photomosaic of three photos

the initial approximations for multiphoto matching, we ensure the selection of areas of sufficient radiometric variation which inherently lead to better matching accuracy. In addition, these areas will most likely correspond to features of interest in the object space, since gray level variations are caused by markings on the ground, and changes in radiance and/or surface orientation. The use of least squares techniques for matching provides the additional advantage of producing results with objectively estimable accuracy, allowing for the proper assignment of weights. Observations in windows of low entropy, which are typically susceptible to erroneous matches can be assigned smaller weights, thus minimizing their effect in a global solution.

In conclusion, it is obvious that multiple image matching is an essential tool in digital photogrammetry. The introduction of geometric constraints and its performance in the object space can contribute to making it more rigorous in theory and consequently practically improved. Combined as discussed with already developed modules, such as stereomatching, it can fully automate the aerotriangulation procedure, and significantly assist in upgrading the mapping process.

References

[1] Ackermann, F. (1984) *Digital Image Correlation: Performance and Potential Application in Photogrammetry*, Photogrammetric Record, Vol. 11, No. 64, pp. 429-439.

[2] Grün, A. & E. Baltsavias (1988) *Geometrically Constrained Multiphoto Matching*, Photogrammetric Engineering & Remote Sensing, Vol. 54, No. 5, pp. 633-641.

[3] Heipke, C. (1992) *A Global Approach for Least-Squares Image Matching and Surface Reconstruction in Object Space*, Photogrammetric Engineering & Remote Sensing, Vol. 58, No. 3, pp. 317-323.

[4] Helava, U.V. (1988) *Object-Space Least-Squares Correlation*, Photogrammetric Engineering & Remote Sensing, Vol. 54, No. 6, pp. 711-714.

[5] Horn, B.K.P. (1986) *Robot Vision*, MIT Press, McGraw-Hill Book Co., 1986.

[6] Lemmens, M.J.P.M. (1988) *A Survey on Stereo Matching Techniques*, International Archives of Photogrammetry and Remote Sensing, Kyoto, Japan, Vol. 27, Part B8, pp.V11-V23.

[7] Pertl, A. (1985) *Digital Image Correlation with an Analytical Plotter*, Photogrammetria, Vol. 40, No. 1, pp. 9-19.

[8] Schenk, A.F., J.C. Li & C. Toth (1991) *Towards an Autonomous System for Orienting Digital Stereopairs*, Photogrammetric Engineering & Remote Sensing, Vol. 57, No. 8, pp. 1057-1064.

[9] Schenk, A.F. & C. Toth (1992) *Reconstructing Small Surface Patches from Multiple Images*, International Archives of Photogrammetry & Remote Sensing, ISPRS XVII Congress, Washington, D.C..

[10] Stefanidis, A., P. Agouris & A.F. Schenk (1991) *Aspects of Accuracy in Automatic Orientation*, Proceedings 1991 ASPRS Annual Convention, Baltimore, Vol. 5, pp. 334-343.

[11] Tsingas, V. (1991) *Automatische Aerotriangulation*, Proceedings of the 43rd Photogrammetric Week, Stuttgart, Heft 15, pp. 253-268.